Genome-wide analysis of long non-coding RNA expression profile in porcine circovirus 2-infected intestinal porcine epithelial cell line by RNA sequencing

Manxin Fang [1] , **Yi Yang** [1] , **Naidong Wang** [1] , **Aibing Wang** [1] , **Yanfeng He** [1] , **Jiaoshun Wang** [1] , **You Jiang** [1] , **Zhibang Deng** Corresp. [1]

[1] Hunan Agricultural University, Hunan Provincial Key Laboratory of Protein Engineering in Animal Vaccines, Changsha, Hunan, China

Corresponding Author: Zhibang Deng
Email address: zbangd@hunau.edu.cn

Porcine circovirus-associated disease (PCVAD), which is induced by porcine circovirus type 2 (PCV2), is responsible for severe economic losses. Recently, the role of noncoding RNAs, and in particular, microRNAs (miRNAs), in PCV2 infection has received great attention. However, the role of long noncoding RNA (lncRNA) in PCV2 infection is unclear. Here, for the first time, we describe the expression profiles of lncRNAs in an intestinal porcine epithelial cell line (IPEC-J2) after PCV2 infection, and analyze the features of differently expressed lncRNAs and their potential target genes. After strict filtering of approximately 150 million reads, we identified 13,520 lncRNAs, including 199 lncRNAs that were differentially expressed in non-infected and PCV2-infected cells. Furthermore, *trans* analysis found lncRNA-regulated target genes enriched for specific GO terms ($P < 0.05$), such as DNA binding, RNA binding, and transcription factor activity, which are closely associated with PCV2 infection. In addition, we analyzed the predicted target genes of differentially expressed lncRNAs, including *SOD2*, *TNFAIP3,* and *ARG1*, all of which are involved in infectious diseases. Our study identifies many candidate lncRNAs involved in PCV2 infection and provides new insight into the mechanisms underlying the pathogenesis of PCVAD.

1 **Genome-wide analysis of long non-coding RNA expression profile in porcine circovirus 2-**

2 **infected intestinal porcine epithelial cell line by RNA sequencing**

4 Manxin Fang[a], Yi Yang[a], Naidong Wang[a],Aibing Wang[a], Yanfeng He[a], Jiaoshun Wang[a], You

5 Jiang[a], Zhibang Deng[a],*

7 [a] Hunan Provincial Key Laboratory of Protein Engineering in Animal Vaccines, Hunan

8 Agricultural University, Changsha, Hunan 410128, China

9 * To whom correspondence should be addressed: Zhibang Deng, PhD.

10 E-mail: zbangd@hunau.edu.cn

Abstract

Porcine circovirus-associated disease (PCVAD), which is induced by porcine circovirus type 2 (PCV2), is responsible for severe economic losses. Recently, the role of noncoding RNAs, and in particular, microRNAs (miRNAs), in PCV2 infection has received great attention. However, the role of long noncoding RNA (lncRNA) in PCV2 infection is unclear. Here, for the first time, we describe the expression profiles of lncRNAs in an intestinal porcine epithelial cell line (IPEC-J2) after PCV2 infection, and analyze the features of differently expressed lncRNAs and their potential target genes. After strict filtering of approximately 150 million reads, we identified 13,520 lncRNAs, including 199 lncRNAs that were differentially expressed in non-infected and PCV2-infected cells. Furthermore, *trans* analysis found lncRNA-regulated target genes enriched for specific GO terms ($P < 0.05$), such as DNA binding, RNA binding, and transcription factor activity, which are closely associated with PCV2 infection. In addition, we analyzed the predicted target genes of differentially expressed lncRNAs, including *SOD2, TNFAIP3,* and *ARG1*, all of which are involved in infectious diseases. Our study identifies many candidate lncRNAs involved in PCV2 infection and provides new insight into the mechanisms underlying the pathogenesis of PCVAD.

1. Introduction

Infectious diseases threaten pig production, which is an important source of meat (Karuppannan & Opriessnig 2017). Porcine circovirus type 2 (PCV2) in the family Circoviridae is one of the most important pathogens affecting the pig population (Todd et al. 1991). This small, non-enveloped, and circular DNA virus is the causative agent of porcine circovirus-associated disease (PCVAD), which can manifest as PCV2-systemic disease, porcine dermatitis, nephropathy syndrome, porcine respiratory disease complex, PCV2-enteric disease, reproductive failure, and acute pulmonary edema (Meng 2013; Segales 2012; Segales et al. 2005). Increasing evidence indicates that PCVAD is a disease that causes considerable economic damage (Lekcharoensuk et al. 2004; Segales 2012).

Recent studies showed that noncoding RNAs play important regulatory roles in PCVAD (Hong et al. 2015; Wang et al. 2017). However, studies of PCV2-induced PCVAD have mainly focused on microRNA rather than on long non-coding RNA (lncRNA). The lncRNAs are defined as non-protein-coding transcripts greater than 200 nucleotides in length (Batista & Chang 2013). They play significant roles in cellular activities, such as genome regulation, and cell growth, differentiation, and apoptosis (Batista & Chang 2013; Yang et al. 2013). Furthermore, many viruses, such as influenza virus, enterovirus, and porcine reproductive and respiratory syndrome virus (PRRSV), can alter the expression of lncRNAs (Winterling et al. 2014; Yin et al. 2013; Zeng et al. 2018). Dysregulation of lncRNAs may also lead to diseases in pigs (Gao et al. 2017; Zhou et al. 2014).

No studies have examined the role of swine lncRNAs in PCV2-associated PCVAD. Enteritis is a common clinical manifestation of PCV2 infection because the intestinal mucosa is the initial site of PCV2 infection (Chae 2005; Kim et al. 2004). The intestinal porcine epithelial cell line IPEC-J2 is a non-transformed columnar epithelial cell line that was isolated from the neonatal piglet mid-jejunum by Helen Berschneider and colleagues (Orlando et al. 1989). IPEC-J2 is a well-validated model for studying the processes involved in pathogenic infections in the porcine intestinal epithelium (Arce et al. 2010; Koh et al. 2008; Skjolaas et al. 2007). Thus, in the current study, we

66   evaluated the expression profiles of lncRNAs in an intestinal porcine epithelial cell line (IPEC-J2)

67   after PCV2 infection by RNA sequencing and validated the results by quantitative real-time

68   polymerase chain reaction (qRT-PCR). Moreover, Gene Ontology (GO) and pathway analyses

69   were conducted to identify the biological roles of lncRNAs that were differentially expressed after

70   PCV2 infection. To our knowledge, this is the first study to describe the aberrant lncRNA

71   expression profile in response to PCV2 infection in IPEC-J2.

72

73

74

75

76

77

78

79

80

81

82

83

84

85

86

87

88

89

90

91

92

2. Materials and Methods

2.1. Cell culture and virus

IPEC-J2 cells lines free from porcine circovirus (Guangzhou Jennio Biotech Co., Ltd., China) were used in the present study. Cells were cultured in DMEM-F12 medium supplemented with 5% FBS. All cells were maintained at 37°C in a humidified incubator containing 5% CO_2. Here, IPEC-J2 cells were cultured on 6-well plastic tissue culture plates (Corning, Inc., Corning, NY, USA) at a density of 3×10^5/well. The virus PCV2b (GenBank accession number: KJ867555) used in this work was provided by Hunan Provincial Key Laboratory of Protein Engineering in Animal Vaccines and stored at −80°C. The infectious titer of the PCV2 virus prepared from IPEC-J2 cells was $10^{4.7}$ $TCID_{50}$/ml.

2.2. Virus infection

PCV2 infection was performed as previously described (Yan et al. 2014). IPEC-J2 cells were grown to approximately 85% confluence and washed twice with phosphate-buffered saline (PBS). Next, cells were infected with PCV2 at $3 \times 10^{2.5}$ $TCID_{50}$/ml. After 1 h of adsorption, infected cells were cultured in fresh medium supplemented with 2% FBS. Uninfected cells were used as a negative control. Both the PCV2-infected and uninfected cells were harvested 36 h post-infection and used for total RNA extraction.

2.3. Library preparation and Illumina sequencing

Total RNA was extracted from each cell group using Trizol (Invitrogen, Carlsbad, USA). The RNA amount and purity of each sample was quantified by NanoDrop ND-1000 (NanoDrop, Wilmington, DE, USA) (Table 1). Moreover, the RNA integrity was assessed by Agilent 2100 Bioanalyzer (Agilent, Santa Clara, CA, USA) (Table 1). In this study, RNA with a RIN (RNA integrity number) = 10 was used for library preparation. After reverse transcription, the purified first-strand cDNA was subjected to PCR amplification. The preparation for library and sequencing were performed according to previous studies (Wang et al. 2016) by LC-Bio (Hangzhou, China).

120   Finally, RNA sequencing was assessed by the HiSeq 4000 (Illumina, San Diego, CA, USA) on a

121   150 bp paired-end run.

122

123   *2.4. Quality control*

124   First, raw reads in the FASTA format were processed through in-house Perl scripts. During this

125   step, clean reads (clean data) were obtained by discarding reads either containing adapter or over

126   10% poly-N sequences, and low quality reads (>50% of bases whose Phred scores were <5%).

127   Meanwhile, Q20, Q30, and GC content were calculated for the clean data. All downstream

128   analyses were carried out based on clean reads with high quality.

129

130   *2.5. Mapping to the reference genome*

131   Clean reads were aligned to the porcine reference genome (Sus scrofa 10.2) downloaded from

132   the Genome website using TopHat v2.0.9 run with default parameters (Trapnell et al. 2012).

133

134   *2.6. Transcriptome assembly*

135   The mapped reads of each cell group were assembled using both StringTie (v1.3.3) and

136   Cufflinks (v2.1.1) based on default parameters as previously described (Pertea et al. 2015; Trapnell

137   et al. 2010).

138

139   *2.7. Identification of lncRNAs*

140   In addition to lncRNAs identified by BLAST searches, we also predicted novel lncRNAs from

141   clean reads (Fig.1). Novel putative lncRNAs had to meet three requirements that have also been

142   described previously: 1) transcripts should be longer than 200 bp and contain more than one exon;

143   2) the fragments per kilobase of transcript per million mapped reads (FPKM) score should be more

144   than 0.5; 3) transcripts should have no coding potential. (Ran et al. 2016; Weng et al. 2017). In

145   addition, the FRKM was transformed by the following formula:

146    $$FPKM = \frac{\text{Total exon Fragments}}{\text{Mapped reads (millions)} \times \text{exon length(kb)}}$$

147 To distinguish protein-coding and non-coding sequences effectively, Coding-Non-Coding-

148 Index (CNCI v2) profiles were analyzed independent of known annotations according to the

149 following parameters: length $\geq$ 200 bp and exon $\geq$ 1 and score $\leq$ 0 (Meng 2013; Segales et al. 2005;

150 Sun et al. 2013; Todd et al. 1991). The Coding Potential Calculator (CPC 0.9r2) mainly assesses

151 the extent and quality of the open reading frame (ORF) in transcript sequences and compares it to

152 sequences in a protein sequence database to differentiate coding and non-coding transcripts (Kong

153 et al. 2007). All transcripts with CPC scores $\leq$ -1 were removed. This filtering process yielded

154 transcripts without coding potential that formed our candidate set of lncRNAs and were used for

155 subsequent analysis.

156

157 *2.8. Distribution of lncRNAs along each chromosome*

158 Based on the location with respect to protein-coding genes, lncRNAs are classified into three

159 types: intergenic lncRNAs (lincRNAs), intronic lncRNAs, and anti-sense lncRNAs (Harrow et al.

160 2012; St Laurent et al. 2015). After comparing with known mRNAs via the class_code module in

161 cuffcompare, the putative lncRNAs were separated into these three classes (Yan et al. 2014). Next,

162 all these kinds of lncRNAs were mapped to the porcine genome separately to determine their

163 chromosomal distribution. Briefly, lncRNAs were aligned by short blast, followed by best hit

164 analysis in short 500 kb segments. To evaluate their chromosomal distribution, we used the start

165 sites of lncRNAs in the chromosomes counted in the pig reference genome (Susscrofa10.2).

166

167 *2.9. Target gene prediction*

168 Transcripts without coding potential constituted our candidate set of lncRNAs. Next, coding

169 genes were searched within a range of 10–100 kb upstream or downstream of each candidate

170 lncRNA for the *cis* target gene(Yan et al. 2014; Zhang et al. 2017a). For *trans* interactions, we

171 determined the level gene expression based on Pearson's correlations. Briefly, the Pearson's

172 correlation coefficients (R) between lncRNAs and mRNAs were calculated using the R statistical

173 package, and lncRNA target genes were predicted with R $\geq$ 0.95(Li et al. 2014).

174

175 *2.10. Quantification of gene expression levels*

176   To determine gene expression levels, we calculated the FPKMs for both lncRNAs and coding

177 genes in each cell group using Cuffdiff (v2.1.1) software run with default parameters as previously

178 described (Trapnell et al. 2010).

179

180 *2.11. Differential expression analysis*

181   To determine differential expression in digital transcript or gene expression datasets, we utilized

182 a model based on a negative binomial distribution provided by Cuffdiff software. In addition,

183 transcripts or genes in biological replicates with $P < 0.05$ were classed as differentially expressed.

184 For non-biological replicates, transcripts or genes with $P < 0.05$ and an absolute value of log2 (fold

185 change) more than 1 were assigned as the threshold for significant differential expression.

186 Coverage signals used to generate heatmaps were obtained using heatmaply (a R package) based

187 on the z-score obtained following dimensionality reduction of FPKM values (Galili et al. 2018).

188

189 *2.12. Validation of RNA-Seq data by qRT-PCR*

190   To further confirm the reliability of the RNA-seq data, qRT-PCR assays were performed.

191 Briefly, single-stranded cDNA was generated using the RevertAid kit (Fermentas Life Science,

192 Burlington, ON, Canada) with random primers. Real-time PCR was conducted using the SYBR

193 Green q-PCR SuperMix (Bio-Rad, Hercules, CA, USA). The primers used are listed in Table 2.

194 Subsequently, Ct values were acquired with manual thresholds using the 7500 System SDS

195 software (ABI, USA). Levels of lncRNA expression were normalized to the level of GAPDH

196 expression according to the $\Delta\Delta$CT method. The lncRNA expression levels between different

197 groups were compared using $2^{-\Delta\Delta\text{CT}}$. *P* values < 0.05 were considered statistically significant.

198

199 *2.13. Gene Ontology (GO) and KEGG pathway enrichment analysis*

200   Analysis of GO enrichment for differentially expressed lncRNAs-regulated target genes was

201   performed using the GOseq R package as previously described(Young et al. 2010) . For KEGG

202   pathway enrichment of differentially expressed lncRNA-regulated target genes (Young et al.

203   2010), the KOBAS software program was used as described previously (Mao et al. 2005).

204

205   **3. Results**

206   *3.1. Reads and mapping of RNA-seq in IPEC-J2 cells*

207   Total RNAs without rRNA for 6 samples including mock (IPEC_A1-A, IPEC_A2-A,

208   IPEC_A3-A) and PCV2-infected IPEC-J2 cells (IPEC_B1-B, IPEC_B2-B, IPEC_B3-B) were

209   sequenced. After discarding low-quality and adapter sequences, approximately 100 million clean

210   reads were obtained for each cell group. The percentage of clean reads was approximately 98%

211   (Table S1). Next, clean reads were mapped to the pig reference genome (Susscrofa10.2) using

212   TopHat; > 69% of the clean reads were mapped (Table S2). More than 58% of reads were uniquely

213   mapped, 42% were non-splice reads, and approximately 16% were splice reads (Table S2).

214   Additionally, more than 60% of the reads were located on exons, whereas approximately 13% of

215   the reads were on introns; the remaining reads were in intergenic regions (Fig. 2A-F, Table S3).

216

217   *3.2. Assessing the quality of RNA-seq data*

218   FPKM values were used to measure gene expression levels in IPEC-J2 cells. Based on the

219   distribution profile for all transcripts shown in Fig. 3A, the patterns of expression between the

220   control group (IPEC_A1-A, IPEC_A2-A, IPEC_A3-A) and PCV2 infection group (IPEC_B1-B,

221   IPEC_B2-B, IPEC_B3-B) were similar. The FPKM density in the control and PCV2 infection

222   groups was consistent (Fig. 3B). Importantly, the RNA-Seq Pearson correlation coefficients of

223   transcript levels were greater than 0.84 in the control group and greater than 0.94 in the PCV2

224   infection group, indicating the rationality of the experimental design between these two groups

225   and similarity of expression within the groups (Fig. 3C).

226

227   *3.3. Identification of lncRNAs in IPEC-J2 cells*

228 Reads were assembled using StringTie and selected lncRNAs were spliced using Cufflinks.

229 After these rigorous selections, 13,520 novel lncRNAs were identified, including 10,975

230 lincRNAs, 2,182 intronic lncRNAs, and 301 anti-sense lncRNAs (Fig. S1A, Table S4). To further

231 evaluate whether these lncRNAs had coding potential, we predicted the protein coding potential

232 using CPC and CNCI. The CPC and CNCI scores in the control and PCV2 infection groups were

233 similar, showing only slight differences (Fig. S1B, C). In total, 14,001 non-coding transcripts were

234 predicted by CPC and 13,520 non-coding transcripts were determined using CNCI. Detailed

235 information for the predicted lncRNAs is shown in Table S5. Moreover, lncRNAs were evenly

236 distributed on each chromosome in both the control and PCV2 infection groups (Fig. S2).

237

238 *3.4. Feature comparison of transcripts*

239 To determine the differences between lncRNAs and mRNAs in IPEC-J2 cells, we compared

240 their transcript structure, sequence conservation, and expression levels. The results showed a

241 contrasting distribution tendency of exon number between mRNAs and lncRNAs (Fig. 4A). The

242 distribution of lncRNAs was enriched on one exon term, which differed from that of mRNAs (Fig.

243 4A). Additionally, a large proportion of mRNAs were longer than 1000 base pairs, whereas

244 lncRNAs were generally shorter (Fig. 4B). As expected, most of the lncRNAs contained a

245 comparatively shorter ORF (mean = 61.41) compared to the ORFs in mRNAs (Fig. 4C). Compared

246 to mRNAs, the expression level of lncRNAs was generally lower (Fig. 4D, E).

247

248 *3.5. Characteristics of lncRNA expression levels between the control and PCV2 infection groups*

249 The tentative lncRNAs were quantified by Cuffdiff software using the read count and FPKM

250 analyses. The graphs in Fig. 5A show the lncRNA expression levels in IPEC-J2 cells after PCV2

251 infection; differentially expressed lncRNAs are also shown. There were 132 up-regulated and 67

252 down-regulated lncRNAs ($P < 0.05$) (Fig. 5B, Table S6). The heat map (Fig. 5C) indicates the

253 differentially expressed lncRNAs ($P < 0.05$) between the control group and the PCV2 infection

254 group. Nine lncRNAs, MSTRG.19762.1, MSTRG.1454.1, MSTRG.641.1, MSTRG.31692.1,

255 MSTRG.385.1, MSTRG.2965.1, MSTRG.15360.1, MSTRG.22503.1, and IMSTRG.5484.1, were

256 selected for validation by qRT-PCR, and the results were consistent with the differential

257 expression observed in the heat map (Fig. 6A-I). Particularly, MSTRG.31692.1 was down-

258 regulated by 20-fold (Fig. 6I).

259

260 *3.6. Prediction and functional analysis of differentially expressed lncRNA trans-regulated target*

261 *genes*

262   All reads were assembled into 31,836 transcripts as either mRNAs or lncRNAs. Briefly, there

263 were 18,316 mRNAs, including 623 mRNAs predicted for differentially expressed lncRNA target

264 genes. Of these 623 mRNAs, the expression of 373 mRNAs was altered by >2-fold. Genes can be

265 regulated by lncRNAs in *cis* or in *trans*, and both regulatory mechanisms may play an important

266 role in pathological and biological processes in pigs. Of the 373 differentially expressed genes,

267 362 were lncRNA trans-regulated target genes. Thus, we focused on differentially expressed

268 lncRNA trans-regulated target genes in this study. The list of differentially expressed lncRNA

269 target genes is shown in Table S7.

270   To further evaluate the relationship between lncRNAs and target genes, we mapped the nine

271 validated lncRNAs and their target genes into the lncRNA-mRNA regulatory network (Fig. 7,

272 Table S8). This interaction network was delineated using the Cytoscape software (v3.7.0). From

273 this network, we inferred that lncRNAs may play a central role in PCV2 infection, as they regulate

274 numerous target genes. Additionally, some of these target genes, including *SOD2*, *TNFAIP3*,

275 *ARG1*, *SERPINB2*, *VLDLR*, *HSPA5*, and *LCN2*, are associated with infectious diseases, suggesting

276 that lncRNAs respond to PCV2 infection by regulating these genes.

277   Next, differentially expressed target genes of the lncRNAs in *trans* were subjected to GO

278 enrichment. The histogram in Fig. 8A shows the number of genes for a term distributed across

279 biological processes, cellular components, and molecular functions. The histogram also shows the

280 enriched GO terms of molecular function, including metal ion binding, DNA binding, ATP

281 binding, nucleotide binding, RNA binding, zinc ion binding, nucleic acid binding, identical protein

282 binding, transcription factor activity, sequence-specific DNA binding, and calcium ion binding

283 (Fig. 8A); detailed information is shown in Table S9.

284 Finally, we performed KEGG pathway enrichment for the differentially expressed lncRNA

285 target genes. The 44 critical pathways with low P values (P < 0.05) and 501 genes are shown in

286 Fig. 8B. Briefly, most enriched pathways were related to the TNF signaling pathway, *Salmonella*

287 infection, Pertussis, MAPK signaling pathway, cytokine-cytokine receptor interaction, Influenza

288 A, and Amoebiasis (Table S10).

289

290 **4. Discussion**

291 PCV2 is associated with PMWS and other porcine diseases that have a major negative impact

292 on the global pig industry. In our efforts to characterize non-coding RNAs that may be involved

293 in porcine diseases, we identified 13,520 novel porcine lncRNAs. Similarly, a large number of

294 novel pig lncRNAs was also identified by another group, who predicted 12,867 novel lncRNAs in

295 porcine alveolar macrophages after infection of the HP-PRRSV GSWW15 strain and the North

296 American strain FL-12 (Zhang et al. 2017b). However, these numbers are low compared with those

297 in other animals, and further characterization of porcine lncRNAs is required. The lncRNAs

298 identified here share universal characteristics with other mammals including fewer exons, shorter

299 length and lower expression level than protein-coding genes(Cabili et al. 2011; Ravasi et al. 2006;

300 Ulitsky & Bartel 2013). Thus, although further characterization is required, the present study

301 provides a reference for studying lncRNAs in other species.

302 There is strong evidence that lncRNAs play a clear role in viral infection. For example, lncRNA

303 NRAV (negative regulator of antiviral response) modulates antiviral responses by suppressing the

304 initiation of interferon-stimulated gene transcription (Ouyang et al. 2014). In addition, the

305 upregulation of lncRNA-CMPK2 contributes to the negative regulation of the interferon response

306 (Kambara et al. 2014). To date, the roles of lncRNAs in viral-host interactions during PCV2

307 infection are still unclear. To our knowledge, this is the first report that characterizes the expression

308 profiles of lncRNAs in the non-transformed columnar epithelial cell line IPEC-J2 after PCV2

309 infection. Post PCV2 infection, we identified 199 differentially expressed lncRNAs, which appear

310 to modify genes associated with viral infection, such as *SOD2*, *TNFAIP3*, *ARG1*, *SERPINB2*,

311 *VLDLR*, *HSPA5*, and *LCN2* (Table S11). For example, *TNFAIP3* is involved in influenza A virus

312 infection (Maelfait et al. 2012), whereas *ARG1* suppresses arthritogenic alphavirus infection

313 (Burrack et al. 2015) Therefore, PCV2 infection-associated lncRNAs may modulate viral infection

314 through regulating these targeted genes.

315   The lncRNAs predicted as regulators of genes related to infectious diseases include

316 MSTRG.4625, MSTRG.8436, MSTRG.4146, MSTRG.5886, MSTRG.5870, MSTRG.4146 and

317 MSTRG.4592 (Table S11). However, since every targeted gene is regulated by several lncRNAs

318 (Table S11), further studies are required to determine the mechanism of combinatorial control.

319   Our functional enrichment analysis revealed that processes including DNA binding,

320 transcription factor activity and identical protein binding are closely associated with PCV2

321 infection. Consistent with this, PCV2 induces the activation of transcription factor nuclear factor

322 kappa B (NF-kappa B) by increasing DNA binding activity (Han et al. 2017; Wei et al. 2008).

323 Another study revealed that PCV2 protein ORF4 induces apoptosis by binding to mitochondrial

324 adenine nucleotide translocase 3 (mtANT3)(Lin et al. 2018). These data suggest that lncRNAs

325 may respond to PCV2 infection through regulating DNA binding, transcription factor activity and

326 identical protein binding.

327   The most enriched pathways in PCV2 infection include the TNF signaling pathway, *Salmonella*

328 infection, Pertussis, MAPK signaling pathway, cytokine-cytokine receptor interaction, Influenza

329 A, and Amoebiasis. *Salmonella* infection often occurs concurrently with PCV2-associated disease

330 (Takada-Iwao et al. 2011); thus, lncRNAs involved in PCV2 infection may also play roles in

331 *Salmonella* infection. However, no studies have directly demonstrated the involvement of the other

332 pathways we identified in PCV2 infection. A previous study has demonstrated that PCV2

333 vaccination may protect piglet against PCV2 infection through inducing TNFα production(Koinig

334 et al. 2015). Notably, these pathways, such as the TNF signaling pathway, MAPK signaling

335 pathway, and cytokine-cytokine receptor interactions, play major roles in the host inflammatory

336 response to numerous infectious diseases e, suggesting that swine lncRNAs may contribute to host

337 inflammation during PCV2 infection. Further studies should focus on exploring the underlying

338 mechanisms by which swine lncRNAs affect PCV2 infection. PCV2 is associated with PMWS

339 and other porcine diseases that have a major negative impact on the global pig industry. In our

340 efforts to characterize non-coding RNAs that may be involved in porcine diseases, we identified

341 13,520 novel porcine lncRNAs. Similarly, a large number of novel pig lncRNAs was also

342 identified by another group, who predicted 12,867 novel lncRNAs in porcine alveolar

343 macrophages after infection of the HP-PRRSV GSWW15 strain and the North American strain

344 FL-12 e. However, these numbers are low compared with those in other animals, and further

345 characterization of porcine lncRNAs is required. The lncRNAs identified here share universal

346 characteristics with other mammals including fewer exons, shorter length and lower expression

347 level than protein-coding genese. Thus, although further characterization is required, the present

348 study provides a reference for studying lncRNAs in other species.

349 The lncRNAs predicted as regulators of genes related to infectious diseases include

350 MSTRG.4625, MSTRG.8436, MSTRG.4146, MSTRG.5886, MSTRG.5870, MSTRG.4146 and

351 MSTRG.4592 (Table S11). However, since every targeted gene is regulated by several lncRNAs

352 (Table S11), further studies are required to determine the mechanism of combinatorial control.

353 Our functional enrichment analysis revealed that processes including DNA binding,

354 transcription factor activity and identical protein binding are closely associated with PCV2

355 infection. Consistent with this, PCV2 induces the activation of transcription factor nuclear factor

356 kappa B (NF-kappa B) by increasing DNA binding activity (Han et al. 2017; Wei et al. 2008).

357 Another study revealed that PCV2 protein ORF4 induces apoptosis by binding to mitochondrial

358 adenine nucleotide translocase 3 (mtANT3)(Lin et al. 2018). These data suggest that lncRNAs

359 may respond to PCV2 infection through regulating DNA binding, transcription factor activity and

360 identical protein binding.

361 The most enriched pathways in PCV2 infection include the TNF signaling pathway, *Salmonella*

362 infection, Pertussis, MAPK signaling pathway, cytokine-cytokine receptor interaction, Influenza

363   A, and Amoebiasis. *Salmonella* infection often occurs concurrently with PCV2-associated disease

364   (Takada-Iwao et al. 2011); thus, lncRNAs involved in PCV2 infection may also play roles in

365   *Salmonella* infection. However, no studies have directly demonstrated the involvement of the other

366   pathways we identified in PCV2 infection. A previous study has demonstrated that PCV2

367   vaccination may protect piglet against PCV2 infection through inducing TNF☐ production(Koinig

368   et al. 2015). Notably, these pathways, such as the TNF signaling pathway, MAPK signaling

369   pathway, and cytokine-cytokine receptor interactions, play major roles in the host inflammatory

370   response to numerous infectious diseases (Benedict et al. 2003; Gong et al. 2011; Li et al. 2011;

371   Maegraith & Harinasuta 1953), suggesting that swine lncRNAs may contribute to host

372   inflammation during PCV2 infection. Further studies should focus on exploring the underlying

373   mechanisms by which swine lncRNAs affect PCV2 infection.

374

375   **Conclusions**

376   In summary, the current study reveals candidate lncRNAs associated with PCV2 infection and

377   the cellular signaling pathways that they modulate. These findings could be valuable in designing

378   novel potential strategies to identify the molecular mechanisms underlying PCV2-associated

379   diseases. In turn, this will facilitate the development of antiviral strategies against PCV2 that will

380   benefit animals in the global pig industry.

381

382

383

384   **References**

385   Arce C, Ramirez-Boo M, Lucena C, and Garrido JJ. 2010. Innate immune activation of swine intestinal epithelial cell

386   lines (IPEC-J2 and IPI-2I) in response to LPS from Salmonella typhimurium. *Comp Immunol Microbiol Infect*

387   *Dis* 33:161-174. 10.1016/j.cimid.2008.08.003

388   Batista PJ, and Chang HY. 2013. Long noncoding RNAs: cellular address codes in development and disease. *Cell*

389   152:1298-1307. 10.1016/j.cell.2013.02.012

390   Benedict CA, Banks TA, and Ware CF. 2003. Death and survival: viral regulation of TNF signaling pathways. *Curr Opin*

391   *Immunol* 15:59-65.

392   Burrack KS, Tan JJ, McCarthy MK, Her Z, Berger JN, Ng LF, and Morrison TE. 2015. Myeloid Cell Arg1 Inhibits Control

393   of Arthritogenic Alphavirus Infection by Suppressing Antiviral T Cells. *PLoS Pathog* 11:e1005191.
394   10.1371/journal.ppat.1005191

395   Cabili MN, Trapnell C, Goff L, Koziol M, Tazon-Vega B, Regev A, and Rinn JL. 2011. Integrative annotation of human
396   large intergenic noncoding RNAs reveals global properties and specific subclasses. *Genes Dev* 25:1915-1927.
397   10.1101/gad.17446611

398   Chae C. 2005. A review of porcine circovirus 2-associated syndromes and diseases. *Vet J* 169:326-336.
399   10.1016/j.tvjl.2004.01.012

400   Galili T, O'Callaghan A, Sidi J, and Sievert C. 2018. heatmaply: an R package for creating interactive cluster heatmaps
401   for online publishing. *Bioinformatics* 34:1600-1602. 10.1093/bioinformatics/btx657

402   Gao PF, Guo XH, Du M, Cao GQ, Yang QC, Pu ZD, Wang ZY, Zhang Q, Li M, Jin YS, Wang XJ, Liu H, and Li BG. 2017.
403   LncRNA profiling of skeletal muscles in Large White pigs and Mashen pigs during development. *J Anim Sci*
404   95:4239-4250. 10.2527/jas2016.1297

405   Gong J, Shen XH, Chen C, Qiu H, and Yang RG. 2011. Down-regulation of HIV-1 infection by inhibition of the MAPK
406   signaling pathway. *Virol Sin* 26:114-122. 10.1007/s12250-011-3184-y

407   Han J, Zhang S, Zhang Y, Chen M, and Lv Y. 2017. Porcine circovirus type 2 increases interleukin-1beta and interleukin-
408   10 production via the MyD88-NF-kappa B signaling pathway in porcine alveolar macrophages in vitro. *J Vet*
409   *Sci* 18:183-191. 10.4142/jvs.2017.18.2.183

410   Harrow J, Frankish A, Gonzalez JM, Tapanari E, Diekhans M, Kokocinski F, Aken BL, Barrell D, Zadissa A, Searle S,
411   Barnes I, Bignell A, Boychenko V, Hunt T, Kay M, Mukherjee G, Rajan J, Despacio-Reyes G, Saunders G,
412   Steward C, Harte R, Lin M, Howald C, Tanzer A, Derrien T, Chrast J, Walters N, Balasubramanian S, Pei B,
413   Tress M, Rodriguez JM, Ezkurdia I, van Baren J, Brent M, Haussler D, Kellis M, Valencia A, Reymond A,
414   Gerstein M, Guigo R, and Hubbard TJ. 2012. GENCODE: the reference human genome annotation for The
415   ENCODE Project. *Genome Res* 22:1760-1774. 10.1101/gr.135350.111

416   Hong JS, Kim NH, Choi CY, Lee JS, Na D, Chun T, and Lee YS. 2015. Changes in cellular microRNA expression induced
417   by porcine circovirus type 2-encoded proteins. *Vet Res* 46:39. 10.1186/s13567-015-0172-5

418   Kambara H, Niazi F, Kostadinova L, Moonka DK, Siegel CT, Post AB, Carnero E, Barriocanal M, Fortes P, Anthony DD,
419   and Valadkhan S. 2014. Negative regulation of the interferon response by an interferon-induced long non-
420   coding RNA. *Nucleic Acids Res* 42:10668-10680. 10.1093/nar/gku713

421   Karuppannan AK, and Opriessnig T. 2017. Porcine Circovirus Type 2 (PCV2) Vaccines in the Context of Current
422   Molecular Epidemiology. *Viruses* 9. 10.3390/v9050099

423   Kim J, Ha Y, Jung K, Choi C, and Chae C. 2004. Enteritis associated with porcine circovirus 2 in pigs. *Can J Vet Res*
424   68:218-221.

425   Koh SY, George S, Brozel V, Moxley R, Francis D, and Kaushik RS. 2008. Porcine intestinal epithelial cell lines as a new
426   in vitro model for studying adherence and pathogenesis of enterotoxigenic Escherichia coli. *Vet Microbiol*
427   130:191-197. 10.1016/j.vetmic.2007.12.018

428   Koinig HC, Talker SC, Stadler M, Ladinig A, Graage R, Ritzmann M, Hennig-Pauka I, Gerner W, and Saalmuller A. 2015.
429   PCV2 vaccination induces IFN-gamma/TNF-alpha co-producing T cells with a potential role in protection.
430   *Vet Res* 46:20. 10.1186/s13567-015-0157-4

431   Kong L, Zhang Y, Ye ZQ, Liu XQ, Zhao SQ, Wei L, and Gao G. 2007. CPC: assess the protein-coding potential of
432   transcripts using sequence features and support vector machine. *Nucleic Acids Res* 35:W345-349.
433   10.1093/nar/gkm391

434 Lekcharoensuk P, Morozov I, Paul PS, Thangthumniyom N, Wajjawalku W, and Meng XJ. 2004. Epitope mapping of
435   the major capsid protein of type 2 porcine circovirus (PCV2) by using chimeric PCV1 and PCV2. *J Virol*
436   78:8135-8145. 10.1128/JVI.78.15.8135-8145.2004
437 Li L, Eichten SR, Shimizu R, Petsch K, Yeh CT, Wu W, Chettoor AM, Givan SA, Cole RA, Fowler JE, Evans MM, Scanlon
438   MJ, Yu J, Schnable PS, Timmermans MC, Springer NM, and Muehlbauer GJ. 2014. Genome-wide discovery
439   and characterization of maize long non-coding RNAs. *Genome Biol* 15:R40. 10.1186/gb-2014-15-2-r40
440 Li Y, Zhou H, Wen Z, Wu S, Huang C, Jia G, Chen H, and Jin M. 2011. Transcription analysis on response of swine lung
441   to H1N1 swine influenza virus. *BMC Genomics* 12:398. 10.1186/1471-2164-12-398
442 Lin C, Gu J, Wang H, Zhou J, Li J, Wang S, Jin Y, Liu C, Liu J, Yang H, Jiang P, and Zhou J. 2018. Caspase-Dependent
443   Apoptosis Induction via Viral Protein ORF4 of Porcine Circovirus 2 Binding to Mitochondrial Adenine
444   Nucleotide Translocase 3. *J Virol* 92. 10.1128/JVI.00238-18
445 Maegraith B, and Harinasuta C. 1953. Experimental amoebiasis in the guineapig. *Trans R Soc Trop Med Hyg* 47:582-
446   583.
447 Maelfait J, Roose K, Bogaert P, Sze M, Saelens X, Pasparakis M, Carpentier I, van Loo G, and Beyaert R. 2012. A20
448   (Tnfaip3) deficiency in myeloid cells protects against influenza A virus infection. *PLoS Pathog* 8:e1002570.
449   10.1371/journal.ppat.1002570
450 Mao X, Cai T, Olyarchuk JG, and Wei L. 2005. Automated genome annotation and pathway identification using the
451   KEGG   Orthology   (KO)   as   a   controlled   vocabulary.   *Bioinformatics*   21:3787-3793.
452   10.1093/bioinformatics/bti430
453 Meng XJ. 2013. Porcine circovirus type 2 (PCV2): pathogenesis and interaction with the immune system. *Annu Rev*
454   *Anim Biosci* 1:43-64. 10.1146/annurev-animal-031412-103720
455 Orlando RC, Powell DW, Croom RD, Berschneider HM, Boucher RC, and Knowles MR. 1989. Colonic and esophageal
456   transepithelial potential difference in cystic fibrosis. *Gastroenterology* 96:1041-1048.
457 Ouyang J, Zhu X, Chen Y, Wei H, Chen Q, Chi X, Qi B, Zhang L, Zhao Y, Gao GF, Wang G, and Chen JL. 2014. NRAV, a
458   long noncoding RNA, modulates antiviral responses through suppression of interferon-stimulated gene
459   transcription. *Cell Host Microbe* 16:616-626. 10.1016/j.chom.2014.10.001
460 Pertea M, Pertea GM, Antonescu CM, Chang TC, Mendell JT, and Salzberg SL. 2015. StringTie enables improved
461   reconstruction of a transcriptome from RNA-seq reads. *Nat Biotechnol* 33:290-295. 10.1038/nbt.3122
462 Ran M, Chen B, Li Z, Wu M, Liu X, He C, Zhang S, and Li Z. 2016. Systematic Identification of Long Noncoding RNAs in
463   Immature and Mature Porcine Testes. *Biol Reprod* 94:77. 10.1095/biolreprod.115.136911
464 Ravasi T, Suzuki H, Pang KC, Katayama S, Furuno M, Okunishi R, Fukuda S, Ru K, Frith MC, Gongora MM, Grimmond
465   SM, Hume DA, Hayashizaki Y, and Mattick JS. 2006. Experimental validation of the regulated expression of
466   large numbers of non-coding RNAs from the mouse genome. *Genome Res* 16:11-19. 10.1101/gr.4200206
467 Segales J. 2012. Porcine circovirus type 2 (PCV2) infections: clinical signs, pathology and laboratory diagnosis. *Virus*
468   *Res* 164:10-19. 10.1016/j.virusres.2011.10.007
469 Segales J, Allan GM, and Domingo M. 2005. Porcine circovirus diseases. *Anim Health Res Rev* 6:119-142.
470 Skjolaas KA, Burkey TE, Dritz SS, and Minton JE. 2007. Effects of Salmonella enterica serovar Typhimurium, or serovar
471   Choleraesuis, Lactobacillus reuteri and Bacillus licheniformis on chemokine and cytokine expression in the
472   swine   jejunal   epithelial   cell   line,   IPEC-J2.   *Vet   Immunol   Immunopathol*   115:299-308.
473   10.1016/j.vetimm.2006.10.012
474 St Laurent G, Wahlestedt C, and Kapranov P. 2015. The Landscape of long noncoding RNA classification. *Trends Genet*

475   31:239-251. 10.1016/j.tig.2015.03.007

476 Sun L, Luo H, Bu D, Zhao G, Yu K, Zhang C, Liu Y, Chen R, and Zhao Y. 2013. Utilizing sequence intrinsic composition
477   to classify protein-coding and long non-coding transcripts. *Nucleic Acids Res* 41:e166. 10.1093/nar/gkt646

478 Takada-Iwao A, Nakanishi M, Souma J, Chikata S, Okuda Y, Imai Y, and Sato S. 2011. Porcine circovirus type 2
479   potentiates morbidity of Salmonella enterica serovar Choleraesuis in Cesarean-derived, colostrum-deprived
480   pigs. *Vet Microbiol* 154:104-112. 10.1016/j.vetmic.2011.06.036

481 Todd D, Niagro FD, Ritchie BW, Curran W, Allan GM, Lukert PD, Latimer KS, Steffens WL, 3rd, and McNulty MS. 1991.
482   Comparison of three animal viruses with circular single-stranded DNA genomes. *Arch Virol* 117:129-135.

483 Trapnell C, Roberts A, Goff L, Pertea G, Kim D, Kelley DR, Pimentel H, Salzberg SL, Rinn JL, and Pachter L. 2012.
484   Differential gene and transcript expression analysis of RNA-seq experiments with TopHat and Cufflinks. *Nat*
485   *Protoc* 7:562-578. 10.1038/nprot.2012.016

486 Trapnell C, Williams BA, Pertea G, Mortazavi A, Kwan G, van Baren MJ, Salzberg SL, Wold BJ, and Pachter L. 2010.
487   Transcript assembly and quantification by RNA-Seq reveals unannotated transcripts and isoform switching
488   during cell differentiation. *Nat Biotechnol* 28:511-515. 10.1038/nbt.1621

489 Ulitsky I, and Bartel DP. 2013. lincRNAs: genomics, evolution, and mechanisms. *Cell* 154:26-46.
490   10.1016/j.cell.2013.06.020

491 Wang X, Xu X, Wang W, Yu Z, Wen L, He K, and Fan H. 2017. MicroRNA-30a-5p promotes replication of porcine
492   circovirus type 2 through enhancing autophagy by targeting 14-3-3. *Arch Virol* 162:2643-2654.
493   10.1007/s00705-017-3400-7

494 Wang Y, Xue S, Liu X, Liu H, Hu T, Qiu X, Zhang J, and Lei M. 2016. Analyses of Long Non-Coding RNA and mRNA
495   profiling using RNA sequencing during the pre-implantation phases in pig endometrium. *Sci Rep* 6:20238.
496   10.1038/srep20238

497 Wei L, Kwang J, Wang J, Shi L, Yang B, Li Y, and Liu J. 2008. Porcine circovirus type 2 induces the activation of nuclear
498   factor kappa B by IkappaBalpha degradation. *Virology* 378:177-184. 10.1016/j.virol.2008.05.013

499 Weng B, Ran M, Chen B, He C, Dong L, and Peng F. 2017. Genome-wide analysis of long non-coding RNAs and their
500   role in postnatal porcine testis development. *Genomics* 109:446-456. 10.1016/j.ygeno.2017.07.001

501 Winterling C, Koch M, Koeppel M, Garcia-Alcalde F, Karlas A, and Meyer TF. 2014. Evidence for a crucial role of a host
502   non-coding RNA in influenza A virus replication. *RNA Biol* 11:66-75. 10.4161/rna.27504

503 Yan M, Zhu L, and Yang Q. 2014. Infection of porcine circovirus 2 (PCV2) in intestinal porcine epithelial cell line (IPEC-
504   J2) and interaction between PCV2 and IPEC-J2 microfilaments. *Virol J* 11:193. 10.1186/s12985-014-0193-0

505 Yang L, Lin C, Jin C, Yang JC, Tanasa B, Li W, Merkurjev D, Ohgi KA, Meng D, Zhang J, Evans CP, and Rosenfeld MG.
506   2013. lncRNA-dependent mechanisms of androgen-receptor-regulated gene activation programs. *Nature*
507   500:598-602. 10.1038/nature12451

508 Yin Z, Guan D, Fan Q, Su J, Zheng W, Ma W, and Ke C. 2013. lncRNA expression signatures in response to enterovirus
509   71 infection. *Biochem Biophys Res Commun* 430:629-633. 10.1016/j.bbrc.2012.11.101

510 Young MD, Wakefield MJ, Smyth GK, and Oshlack A. 2010. Gene ontology analysis for RNA-seq: accounting for
511   selection bias. *Genome Biol* 11:R14. 10.1186/gb-2010-11-2-r14

512 Zeng N, Wang C, Liu S, Miao Q, Zhou L, Ge X, Han J, Guo X, and Yang H. 2018. Transcriptome Analysis Reveals Dynamic
513   Gene Expression Profiles in Porcine Alveolar Macrophages in Response to the Chinese Highly Pathogenic
514   Porcine Reproductive and Respiratory Syndrome Virus. *Biomed Res Int* 2018:1538127.
515   10.1155/2018/1538127

516 Zhang G, Duan A, Zhang J, and He C. 2017a. Genome-wide analysis of long non-coding RNAs at the mature stage of

517   sea buckthorn (Hippophae rhamnoides Linn) fruit. *Gene* 596:130-136. 10.1016/j.gene.2016.10.017

518 Zhang J, Sun P, Gan L, Bai W, Wang Z, Li D, Cao Y, Fu Y, Li P, Bai X, Ma X, Bao H, Chen Y, Liu Z, and Lu Z. 2017b.

519   Genome-wide analysis of long noncoding RNA profiling in PRRSV-infected PAM cells by RNA sequencing. *Sci*

520   *Rep* 7:4952. 10.1038/s41598-017-05279-z

521 Zhou ZY, Li AM, Adeola AC, Liu YH, Irwin DM, Xie HB, and Zhang YP. 2014. Genome-wide identification of long

522   intergenic noncoding RNA genes and their potential association with domestication in pigs. *Genome Biol*

523   *Evol* 6:1387-1392. 10.1093/gbe/evu113

524

525 **Figure legends**

526 **Figure 1. The pipeline for identifying putative lncRNAs.** Briefly, 55,463 transcripts were

527 assembled and 13,520 novel lncRNAs were identified.

528

529 **Figure 2. Region distribution of raw reads**. The summary of the region distribution of raw reads

530 in the genome from the control groups IPEC_A1-A (A), IPEC_A2-A (B), IPEC_A3-A (C) and

531 PCV2 infection groups IPEC_B1-B (D), IPEC_B2-B (E), IPEC_B3-B (F).

532

533 **Figure 3. Reads and results of mapping RNA identified by deep sequencing.** (A) The FPKM

534 distribution is shown as a box plot. (B) FPKM density distribution for all transcripts. (C) Pearson

535 correlation coefficients for all samples.

536

537 **Figure 4. Comparison between lncRNAs and mRNAs.** LncRNA and mRNA transcripts

538 compared by exon number (A), length (B), ORF length (C), and expression level (D and E).

539

540 **Figure 5. Characteristics of lncRNA expression levels between PCV2-infected and control**

541 **groups**. All lncRNA expression levels are shown; differentially expressed lncRNAs are shown in

542 red (up-regulated) or blue (down-regulated) (A). The number of differentially expressed lncRNAs

543 (B). Heat map showing the expressed lncRNAs (P < 0.05) in the two groups. Colors from dark

544 blue to orange stand for z-score passed the dimensionality reduction of FPKM value filter and

545 reveal increasing RNA levels in each group (C).

546

547 **Figure 6. Validation of RNA-Seq data by qRT-PCR.** Left Y-axis shows the FPKM values of

548 the selected lncRNAs (A-I) using RNA-seq, whereas the right Y-axis shows the relative expression

549 levels of selected lncRNAs (A-I) using qPCR. * indicates P ＜0.05.

550

551 **Figure 7. Regulatory lncRNA-mRNA network based on validated lncRNAs and target genes.**

552 View of the lncRNA-mRNA regulatory network according to nine validated lncRNAs and their

553 target genes.

554

555 **Figure 8. Functional analysis of target genes regulated by differentially expressed**

556 **lncRNAs in *trans*.** For *trans* interactions, the GO enrichment histogram (A), GO terms (B), and

557 KEGG pathway enrichment scatter plot (B) are shown.

558

559

Figure 1

The developed pipeline for identifying putative lncRNAs.

Briefly, 55,463 transcripts were assembled and 13,520 novel lncRNAs were identified.
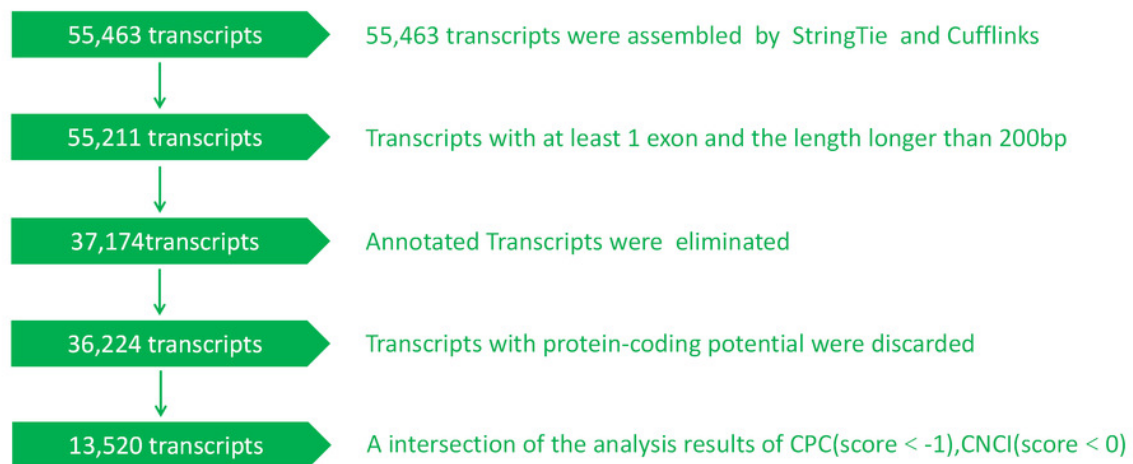
Figure 2

Region distribution of raw reads.

The summary of the region distribution of raw reads in the genome from the control groups IPEC_A1-A (A), IPEC_A2-A (B), IPEC_A3-A (C) and PCV2 infection groups IPEC_B1-B (D), IPEC_B2-B (E), IPEC_B3-B (F).
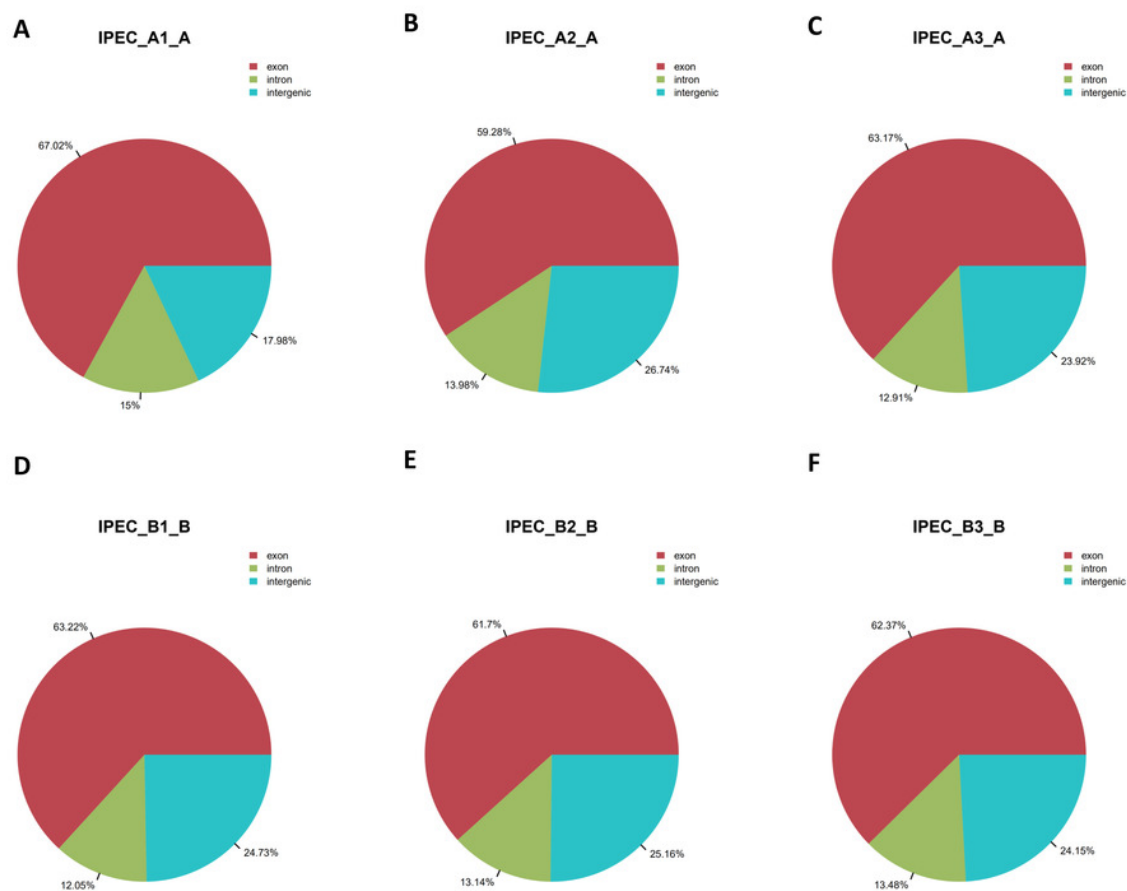
Figure 3

Reads and mapping results of RNA deep sequencing.

(A) The FPKM distribution is shown as a box plot. (B) FPKM density distribution for all transcripts. (C) Pearson correlation coefficients for all samples.
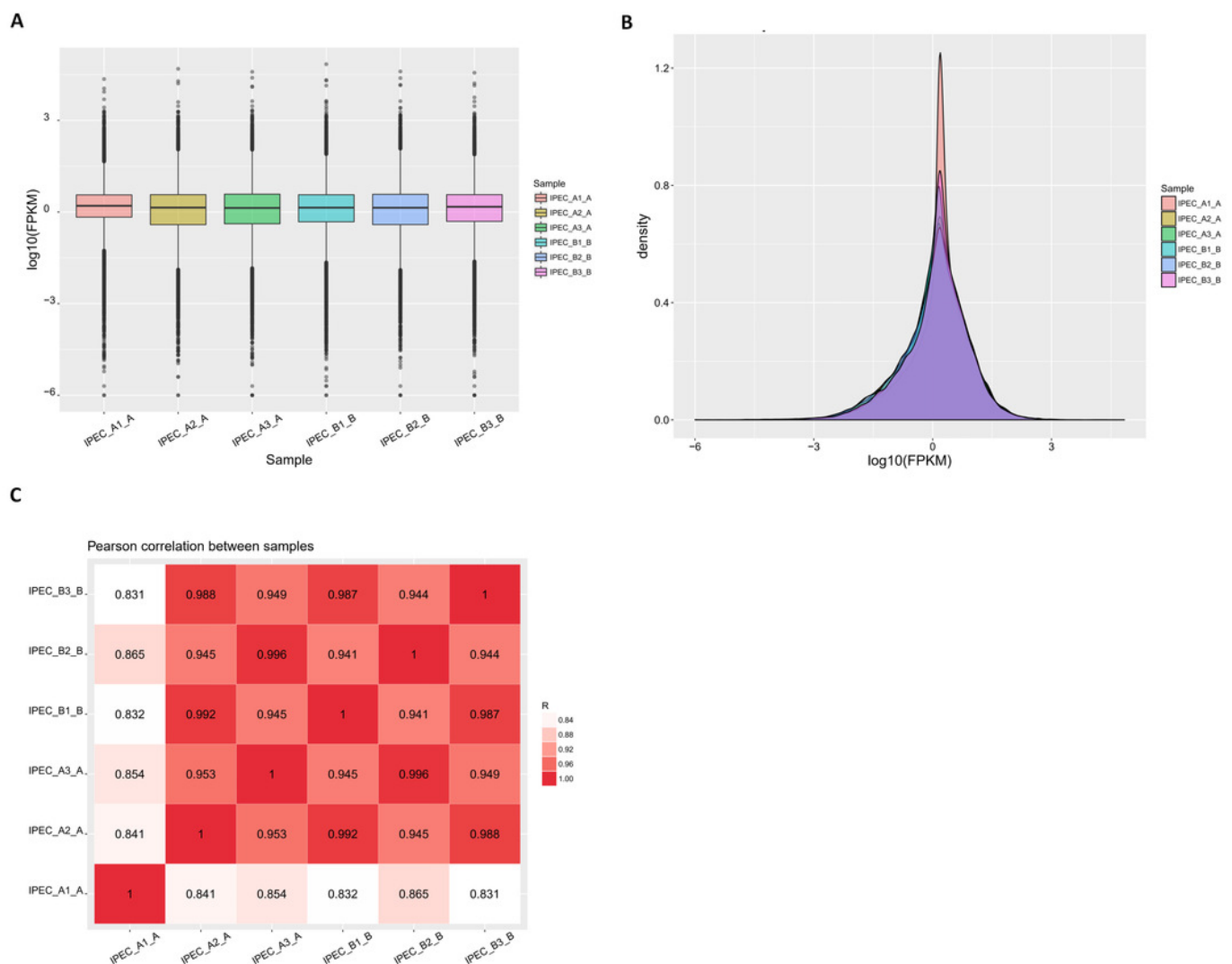
Figure 4

Comparison between lncRNAs and mRNAs.

LncRNA and mRNA transcripts compared by exon number (A), length (B), ORF length (C), and expression level (D and E).
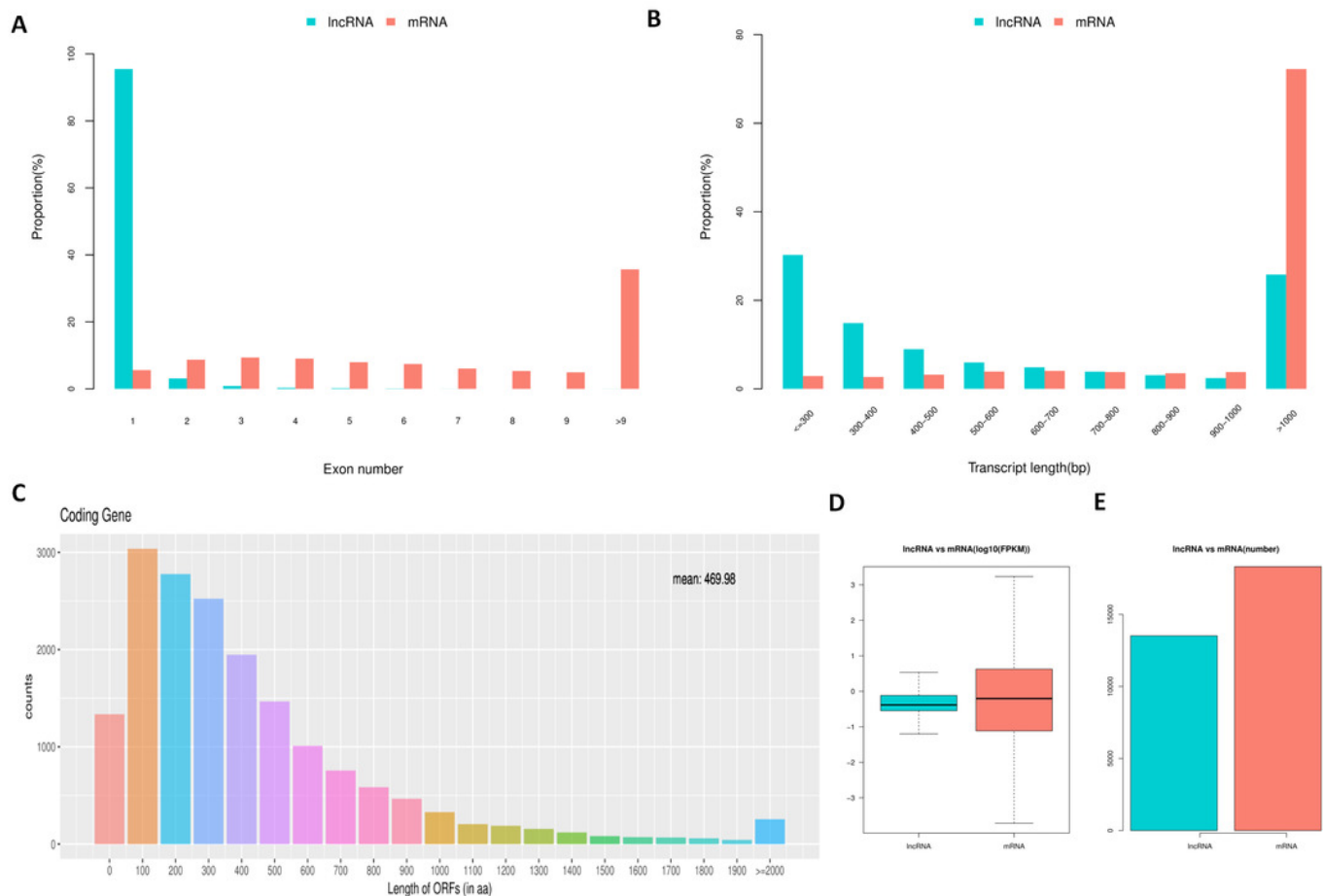
Figure 5

Characteristics of lncRNA expression levels between PCV2 infection and control groups.

All lncRNA expression levels are shown; differentially expressed lncRNAs are shown in red (up-regulated) or blue (down-regulated) (A). Number of differentially expressed lncRNAs (B). Heat map showing the expressed lncRNAs (P < 0.05) in the two groups. Colours from dark blue to orange reveal increasing RNA levels in each group (C).
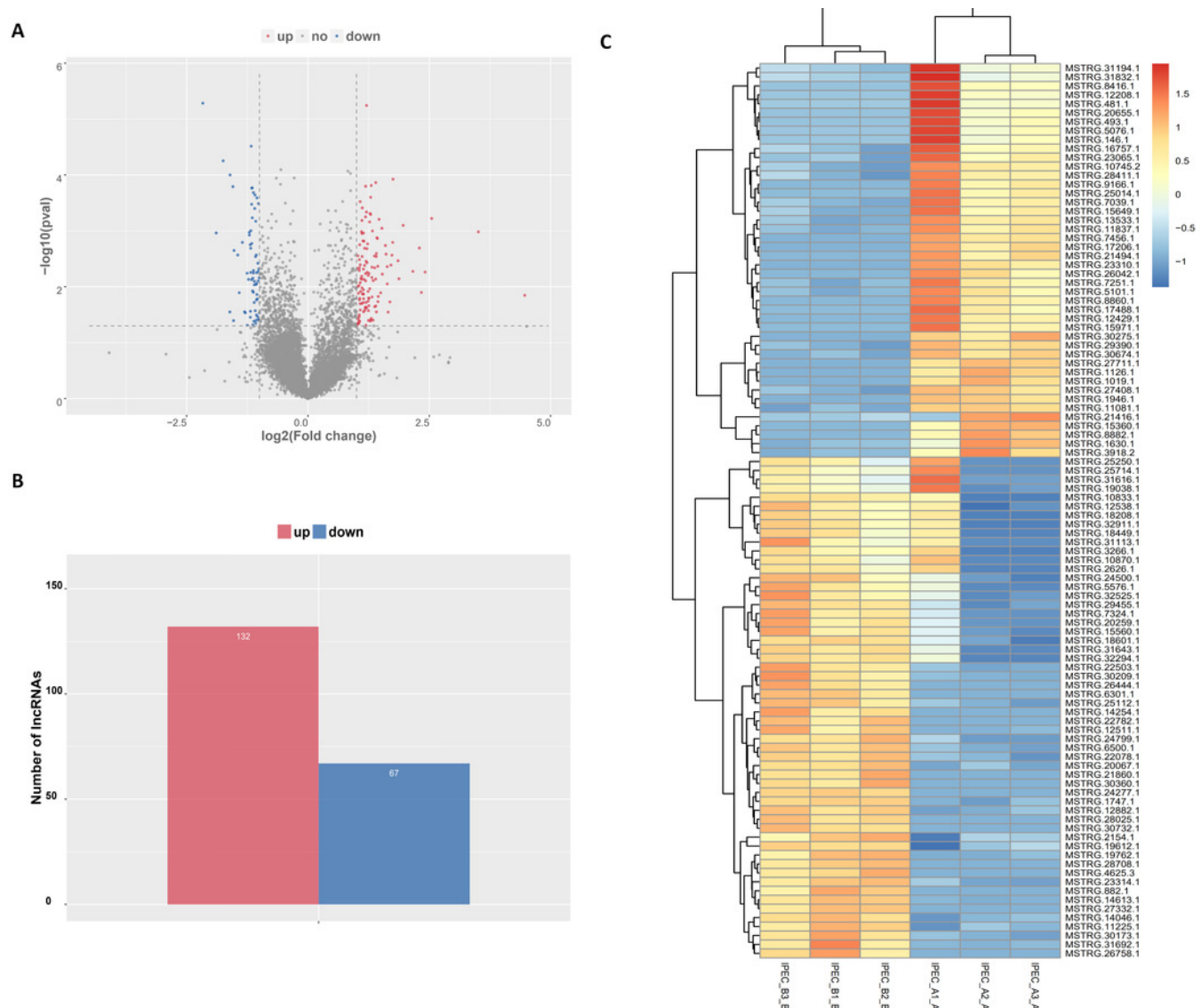
Figure 6

Validation of RNA-Seq data by qRT-PCR.

Left Y-axis shows the FPKM values of the selected lncRNAs (A-I) using RNA-seq, whereas the right Y-axis shows the relative expression levels of selected lncRNAs (A-I) using qPCR. * indicates P ⬚ 0.05.
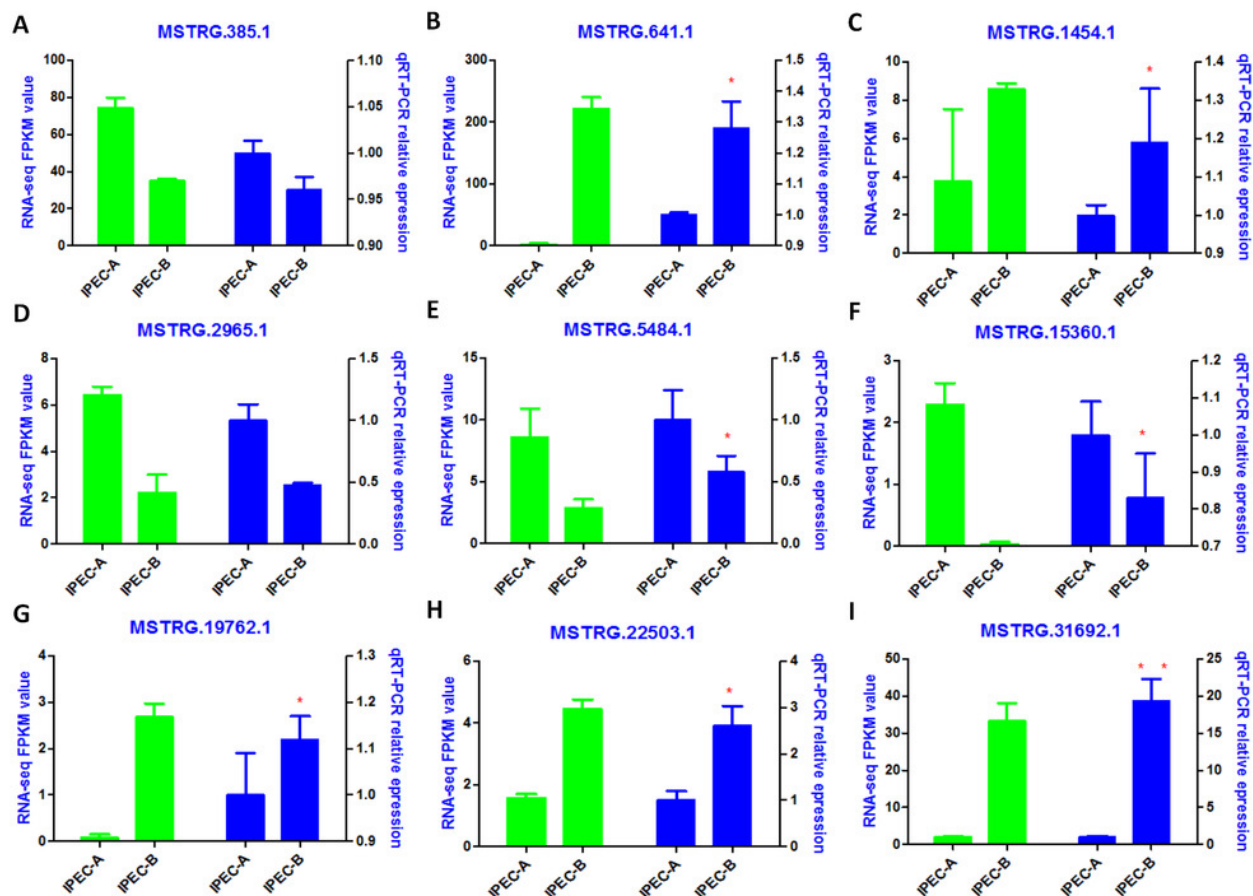
Figure 7

LncRNA-mRNA regulatory network between validated lncRNAs and target genes.

View of lncRNA-mRNA regulatory network according to nine validated lncRNAs and their target genes.
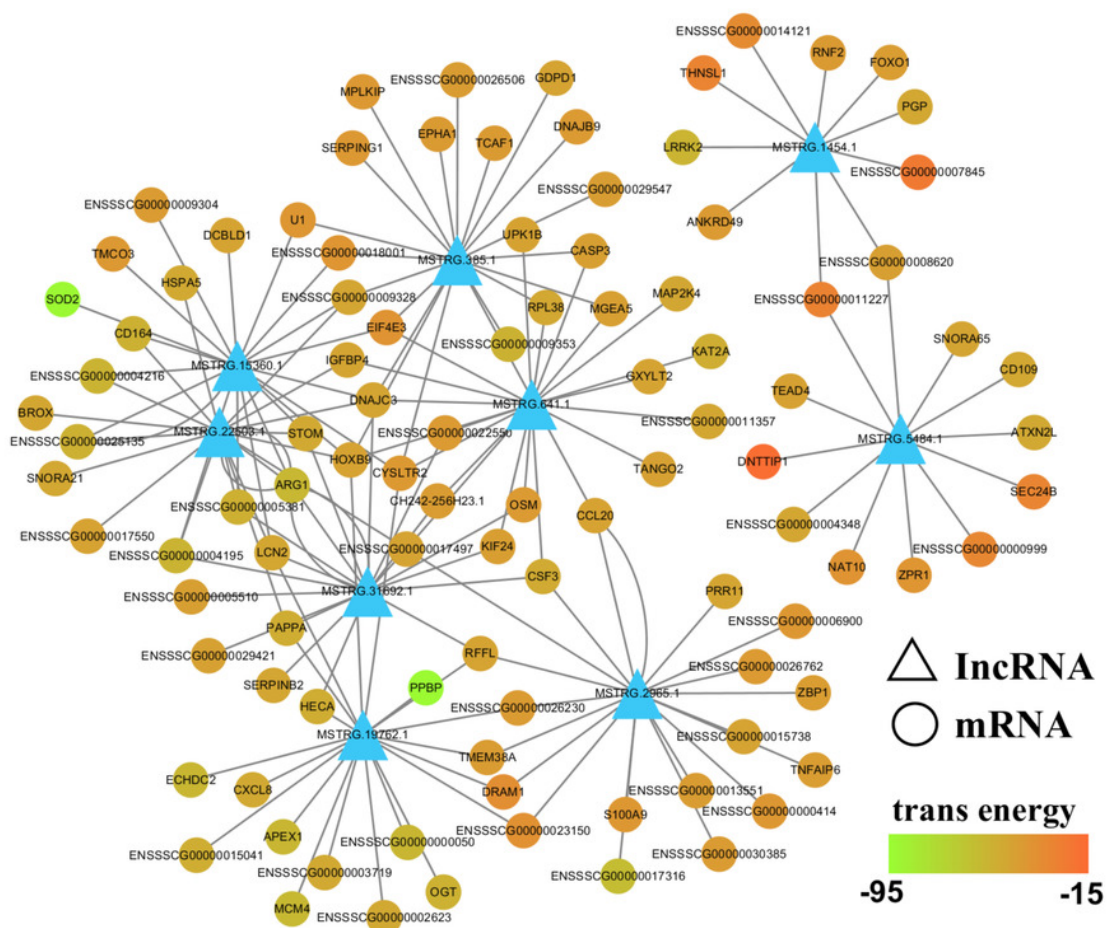
Figure 8

Functional analysis of target genes regulated by differentially expressed lncRNAs in *trans.*

For *trans* interactions, the GO enrichment histogram (A), GO terms (B), and KEGG pathway enrichment scatter plot (B) are shown.
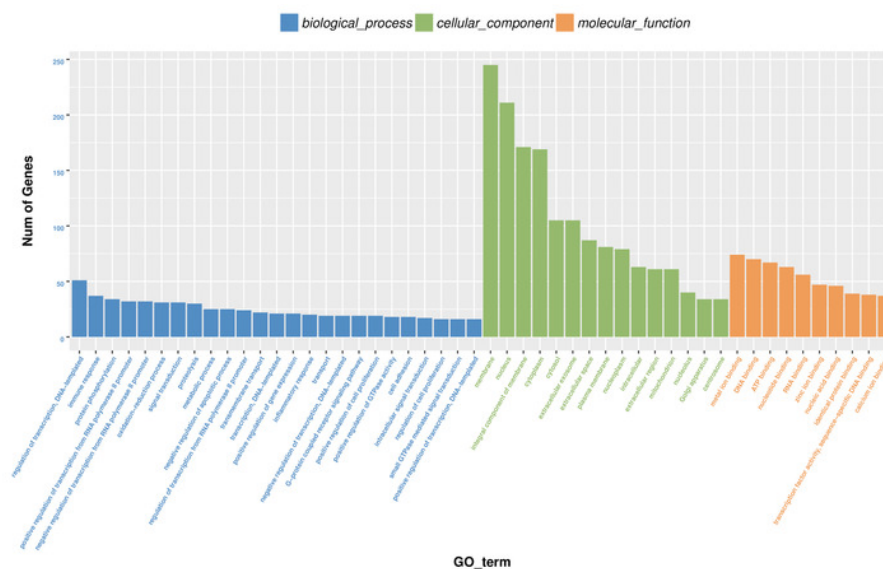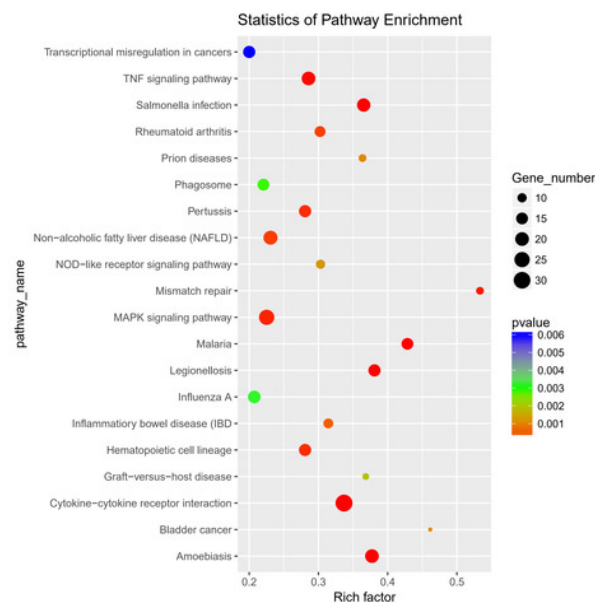
Quality of total RNA

1 **Table 1 Quality of total RNA**

Sample name	Conc.(μg/μL)	Total(μg)	260/280	RIN	28S/18S	QC Evaluation
IPEC-A1-A	2.04	61.32	2.06	10	2.1	A
IPEC-A2-A	1.98	59.31	2.08	10	2.0	A
IPEC-A3-A	2.03	60.82	2.06	10	2.0	A
IPEC-B1-B	1.96	58.93	2.08	10	1.9	A
IPEC-B2-B	1.85	55.62	2.08	10	2.0	A
IPEC-B3-B	2.22	66.48	2.03	10	1.9	A

Primer list

Table 2 Primer list

Gene	ID		Primer sequence	Product length
MSTRG.19762.1		F	CGACGACAAAACGAGAGTCA	196
		R	AATTCTTGAAAAGCGGCTGA	
MSTRG.1454.1		F	CACCTTCTCCATTGCTCCAT	207
		R	CATGCTGCTTTATTGCCAAA	
MSTRG.641.1		F	TGCTCTCGGTCTCCCTTCTA	202
		R	TTGGGATCCTCGACATTCTC	
MSTRG.31692.1		F	CGTGAGAGATGCCATTCAGA	215
		R	AGGACTACCCTCCACCGAGT	
MSTRG.385.1		F	TCCGACTAGGAACCATGAGG	173
		R	TCCCAGGCTAGGGGTCTAAT	
MSTRG.2965.1		F	CTCAGTGGGTTAAGGGTCCA	161
		R	GTTTTCTGGCTGCACATACG	
MSTRG.15360.1		F	ATAAGGTTGCGGGTTCGAT	172
		R	TCCCTCAGCATATGGAGGTT	
MSTRG.22503.1		F	AACCAACTCGGTTGTTCCTG	239
		R	CCTATCGCCTTTCTCTGTGC	
MSTRG.5484.1		F	GAGCCGCATCTGCTACCTAC	207
		R	ACACGGTTCCGGACTTAGTG	
GAPDH	396823	F	TCGGAGTGAACGGATTTGGC	189
		R	TGACAAGCTTCCCGTTCTCC	